
Quantum Sensing, Rev. Mod. Phys. 89, 035002

Chapter III

Examples of Quantum Sensors

A. Neutral Atoms · B. Trapped Ions · C. Rydberg Atoms · D. Atomic Clocks · E. Solid-State Spins (Ensemble)

May 22, 2026 | Yusuke Takeuchi

Chapter III A–E at a Glance

Quantum systems → measured quantities → fundamental-physics examples

- The review classifies quantum sensors by implementation, measured quantity, initialization, and readout.
- I summarize the key points of each implementation and add selected connections to particle / fundamental physics.

Adopted from Table 1

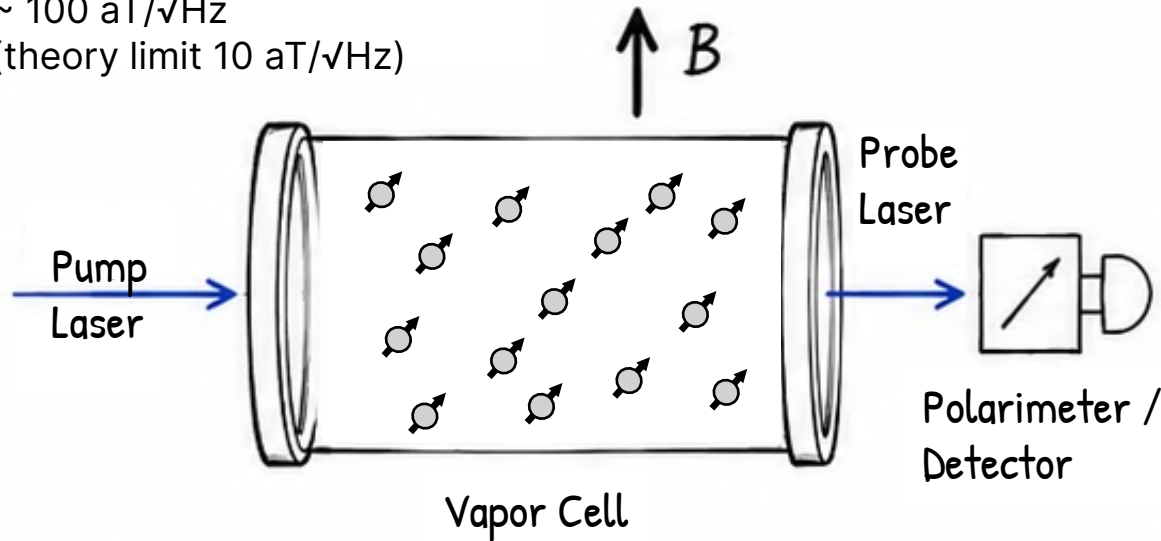
| Section | Implementation | Quantum system | Measured quantity |
|---------|--------------------|--|--|
| III-A | Atomic vapor | atomic spin | magnetic field, rotation |
| III-A | Cold atomic clouds | atomic spin | magnetic field, acceleration |
| III-B | Trapped ions | electronic / spin / vibrational states | rotation, electric field, force |
| III-C | Rydberg atoms | Rydberg states | electric field, including GHz/microwave fields |
| III-D | Atomic clocks | clock transitions | oscillator phase / time/frequency |
| III-E | NMR ensembles | nuclear spins | magnetic field |
| III-E | NV ensembles | electron spins | magnetic field, electric field, temperature |

- Goal:
Compare the sensor implementations in Chapter III A–E by their quantum system, measured quantity, limitations, and selected fundamental-physics applications.

Atomic Vapors

Spin precession in an optically pumped vapor

The most sensitive magnetometers to date
 $\sim 100 \text{ aT}/\sqrt{\text{Hz}}$
 (theory limit $10 \text{ aT}/\sqrt{\text{Hz}}$)



Magnetic-field-sensitive spin precession

Main sensing quantities:

- **Magnetic field B**
 \rightarrow Larmor precession ($\omega_L = \gamma B$)
- **Rotation Ω**
 \rightarrow Rotation-induced spin precession ($\omega_\Omega \simeq \Omega$)

Key characteristics:

- **Collective spin-phase sensing**
 The ensemble phase is the sensing variable.
- **Large atomic ensembles**
 Typically, 10^9 – 10^{12} polarized atoms \rightarrow projection noise $\propto 1/\sqrt{N}$
- **Long spin coherence**
 Coherence times from ms to s \rightarrow long phase accumulation time
- **SERF operation in near-zero magnetic fields**
 Spin-exchange relaxation strongly suppressed
 \rightarrow enables long coherence and high sensitivity

Practical issue:

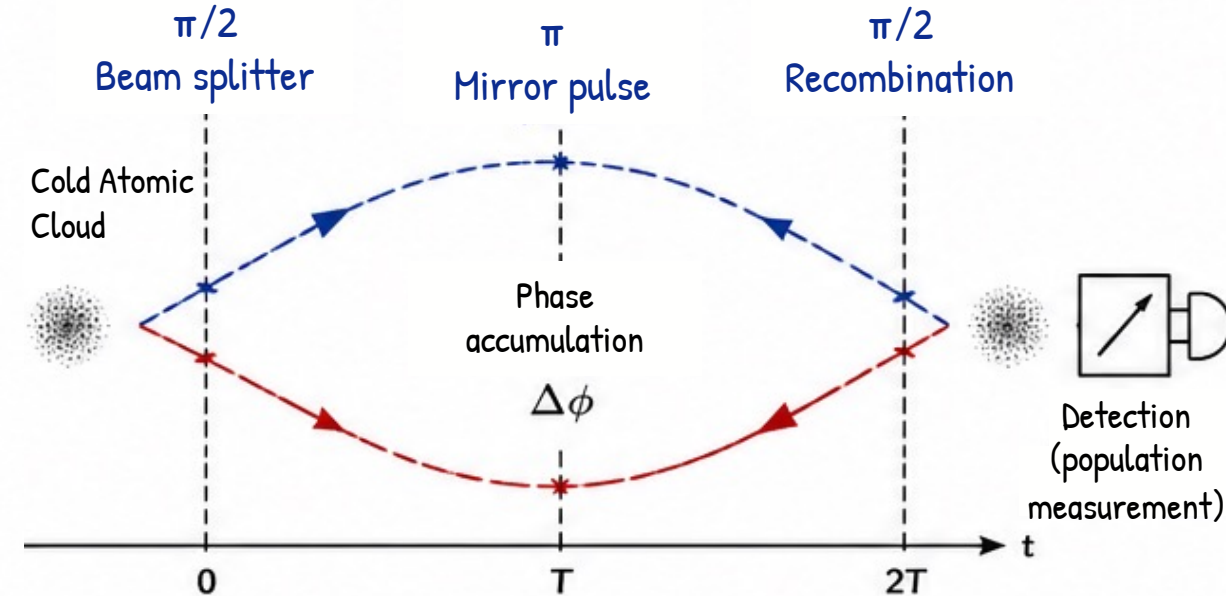
- Best sensitivity often requires near-zero field, magnetic shielding, and careful control of gradients / light shifts

Particle physics applications (examples):

- **Spin-dependent exotic interactions [Exp: 1]**
 \rightarrow effective pseudo-magnetic fields
- **Lorentz / CPT violation with ^{21}Ne – Rb – K comagnetometer [Exp: 2]**
 \rightarrow anomalous spin precession
- **Axion-like dark matter with SERF comagnetometer [Exp: 3]**
 \rightarrow oscillating pseudo-fields
- **Magnetometry for neutron EDM experiments [Exp: 4]**
 \rightarrow ultra-precise magnetic-field control (co-magnetometry)

Cold Atomic Clouds

Matter-wave phase as a probe of acceleration



Acceleration-sensitive matter-wave phase

Main sensing quantities:

- **Acceleration a**
→ Inertial matter-wave phase shift ($\Delta\phi_a = k_{\text{eff}} a T^2$)

Key characteristics:

- **Matter-wave phase sensing**
Interferometric phase is the sensing variable.
- **Long interrogation time**
Cold atoms enable long free-fall or trapped evolution
→ large phase accumulation
- **Small velocity spread**
Laser cooling reduces thermal motion and Doppler noise
→ high phase stability
- **High sensitivity to acceleration**
Phase scales as T^2 for acceleration
→ excellent inertial sensitivity

Practical issue:

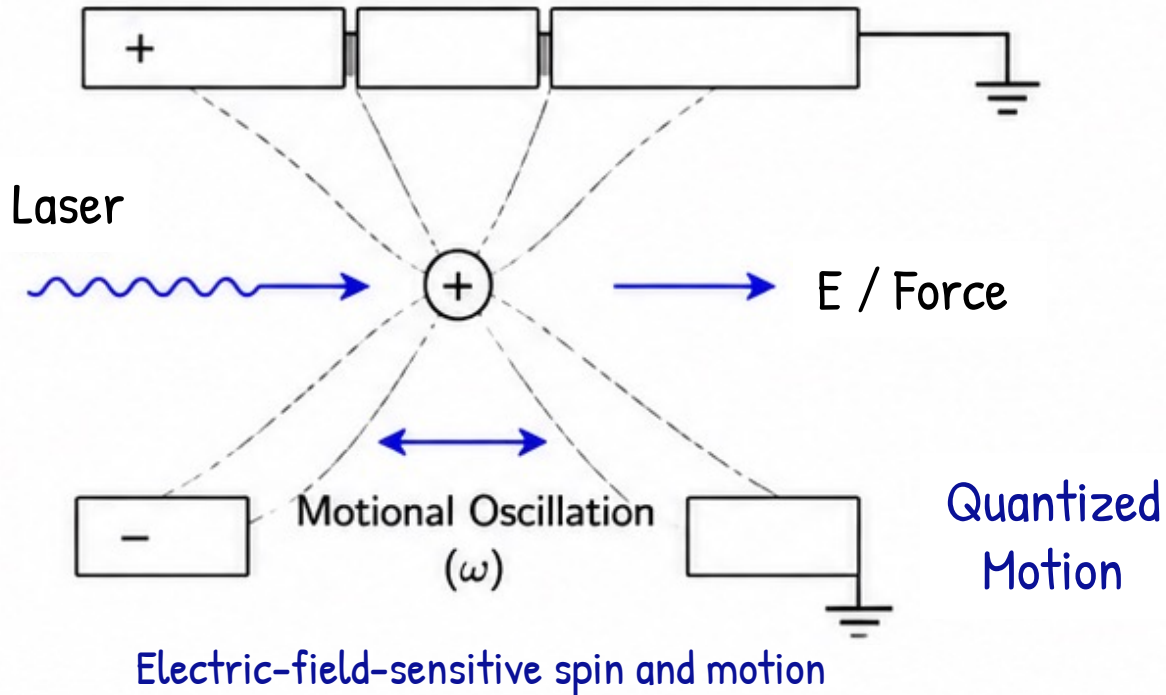
- Best sensitivity requires: Maybe expensive
ultrahigh vacuum, stable lasers, and vibration control

Particle physics applications (examples):

- **Equivalent-principle tests with atom interferometry [Exp: 5]**
→ differential acceleration measurements
- **Fine-structure constant from atom-recoil interferometry [Exp: 6]**
→ precise determination via recoil phase
- **QED / electron $g-2$ consistency test via α [Exp: 6]**
→ recoil frequency and mass measurements
- **Long-baseline atom interferometers for DM/GW searches [Prop: 7,8]**
→ sensitive to phase oscillations/transients

Trapped Ions

Clean, controllable quantum probes in vacuum



Main sensing quantities:

- **Electric field E / force**
→ motional excitation of trapped ions
- **Magnetic field B**
→ spin-state energy splitting / phase evolution
- **Rotation**
→ matter-wave Sagnac phase shift

Key characteristics:

- **Quantized motional states**
Sensitive to weak electric fields and forces.
- **Magnetic-field-sensitive spin states**
Ground-state spin sublevels act as magnetic-field-sensitive qubits.
- **Extremely clean isolated quantum system**
Ultra-low environmental decoherence in vacuum.
- **Excellent coherent control**
Internal and motional states can be precisely manipulated.

Practical issue:

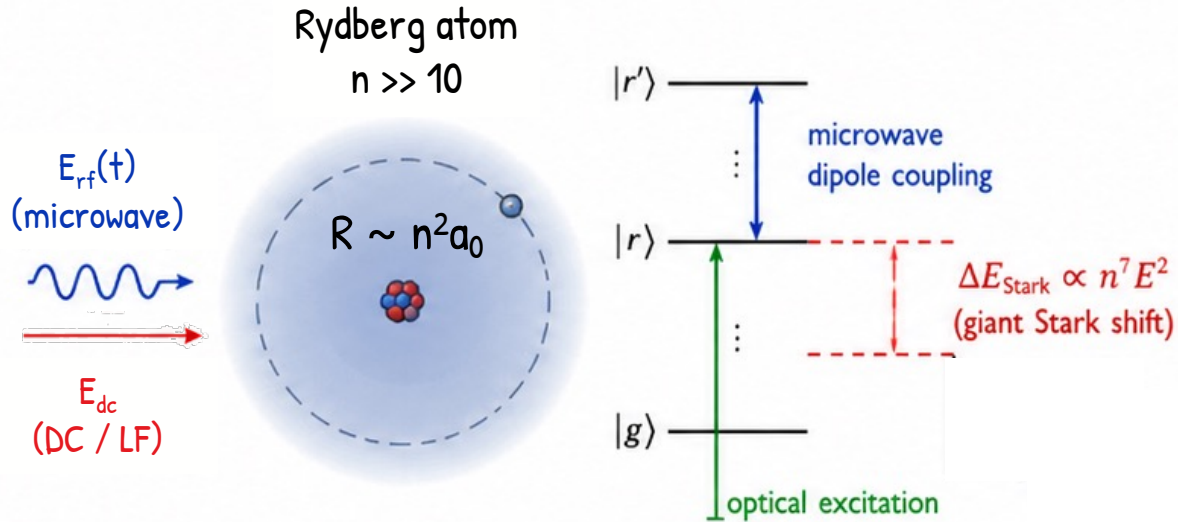
- Surface electric-field noise causes decoherence.
- Single-ion sensitivity is limited compared with ensemble sensors
- Operation close to surfaces remains challenging.

Particle physics applications (examples):

- **Light DM detection with trapped-ion motional states [Prop: 9]**
→ weak DM-induced electric fields drive vibrational excitation
- **Fifth-force / new-boson bounds with Ca^+ isotope shifts [Exp: 10]**
→ deviations from expected isotope-shift patterns
- **Lorentz-symmetry tests with trapped Ca^+ ions [Exp: 11]**
→ sidereal modulation of transition frequencies
- **Improved Lorentz-violation bounds with trapped Yb^+ ions [Exp: 12]**
→ ultra-stable frequency comparison

Rydberg Atoms

Large electric dipoles for weak electric and RF fields



Microwave electric-field sensing

Main sensing quantities:

- **Electric field E**
→ Large Stark shift of Rydberg levels ($\Delta E_{Stark} \propto n^7 E^2$)
- **Microwave / RF field E_{rf}**
→ Resonant dipole transitions between Rydberg states ($R \sim n^2 a_0$)

Key characteristics:

- **Huge electric dipole moments**
Dipole moments scale strongly with principal quantum number n .
- **Extremely large polarizability**
→ giant Stark shifts from weak electric fields ($\Delta E \propto n^7 E^2$)
- **Strong microwave / GHz coupling**
Resonant transitions between nearby Rydberg states enable sensitive detection of RF fields.
- **Optical preparation and readout**
Laser excitation and spectroscopy convert RF signals into optical signals for high-sensitivity detection.

Practical issue:

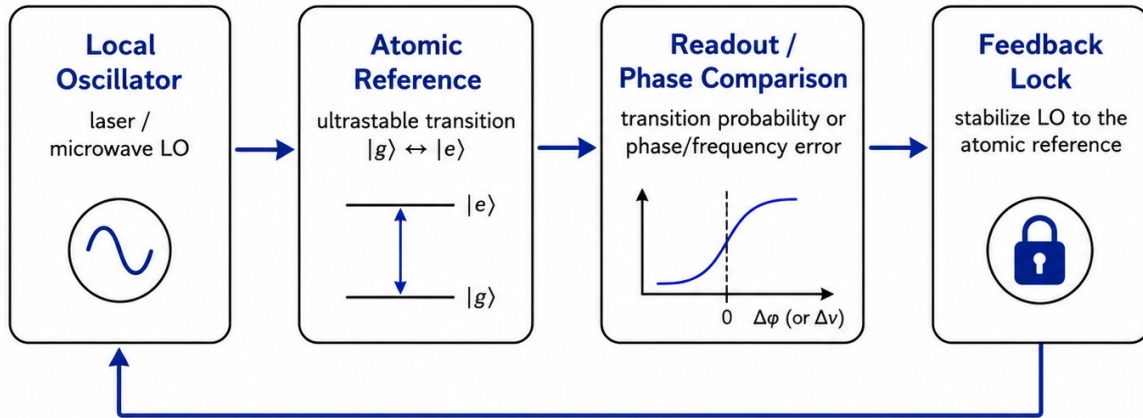
- Extremely sensitive to stray electric fields, surface charges, and field inhomogeneities
- Blackbody-radiation-induced transitions and dephasing broaden the spectroscopy signal
- Cryogenic cavity integration and stable field control are experimentally demanding

Particle physics applications (examples):

- **Axion haloscope readout with Rydberg atoms [Prop: 13]**
→ single microwave-photon detection from axion conversion
- **Dark matter detection with Rydberg tweezer arrays [Prop: 14]**
→ DM-induced electric fields drive transitions between Rydberg states

Atomic Clocks

Frequency references viewed as quantum sensors



Precision frequency comparison

Main sensing quantities:

- Frequency / phase drift

→ repeated comparison between atomic transition and LO

- Tiny transition-frequency shifts

→ caused by external perturbations or new physics

Key characteristics:

- Ultrastable clock transitions

Narrow atomic transitions provide an absolute frequency reference.

- Long coherence and high frequency stability

Long phase accumulation enables precise frequency comparison.

- Optical lattice, trapped-ion, and quantum-logic clocks

State-of-the-art platforms realize optical-frequency precision.

Practical issue:

- Systematic shifts: blackbody radiation, Zeeman / Stark shifts

Environmental perturbations shift the clock transition frequency.

- LO noise, laser stability, and frequency transfer

Clock performance depends on stable interrogation and comparison.

- Complex control of environment and apparatus

Vacuum, temperature, fields, and trapping conditions must be controlled.

Particle physics applications (examples):

- Ultralight dark matter from optical/MW clock comparisons [Exp: 15]

→ oscillating fundamental constants

- Atom-cavity frequency comparison searches [Exp: 16]

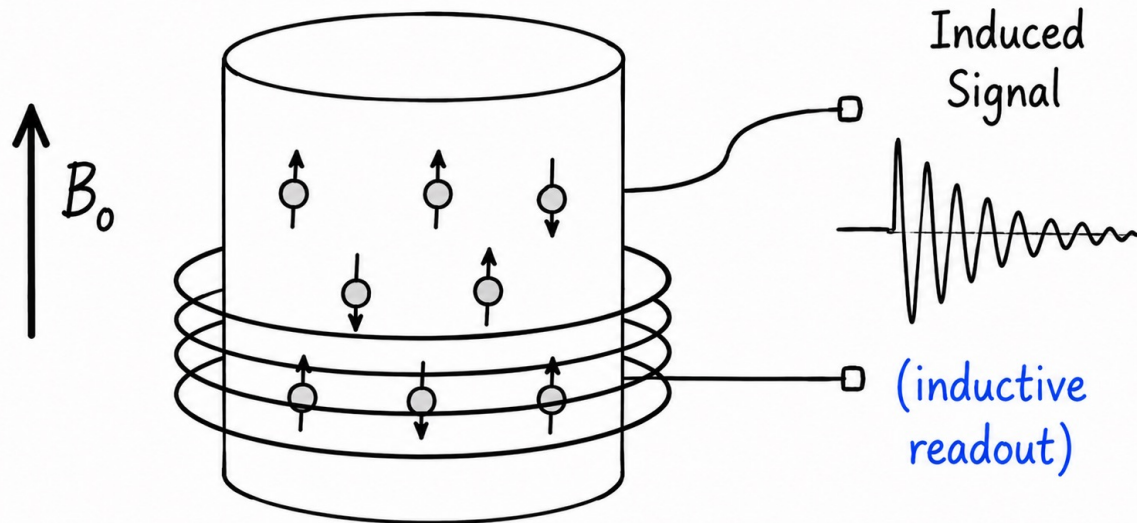
→ dark-matter-induced frequency modulation

- Transient dark matter with clock networks [Prop: 17]

→ correlated timing/frequency excursions across Earth-scale networks

NMR Ensembles

Nuclear-spin precession in robust ensembles



Nuclear-spin precession sensing

Main sensing quantities:

- **Magnetic field B**
→ Larmor precession ($\omega_L = \gamma B$)
- **Rotation Ω**
→ Rotation-induced spin precession ($\omega_\Omega \approx \Omega$)

Key characteristics:

- **Robust nuclear-spin ensembles**
Weak environmental coupling → stable operation
- **Long spin coherence**
Nuclear spins can maintain coherence for long durations
- **Mature low-noise detection techniques**
High-Q inductive detection and precision RF techniques
- **Natural platform for precision precession measurements**
Direct frequency-based sensing

Practical issue:

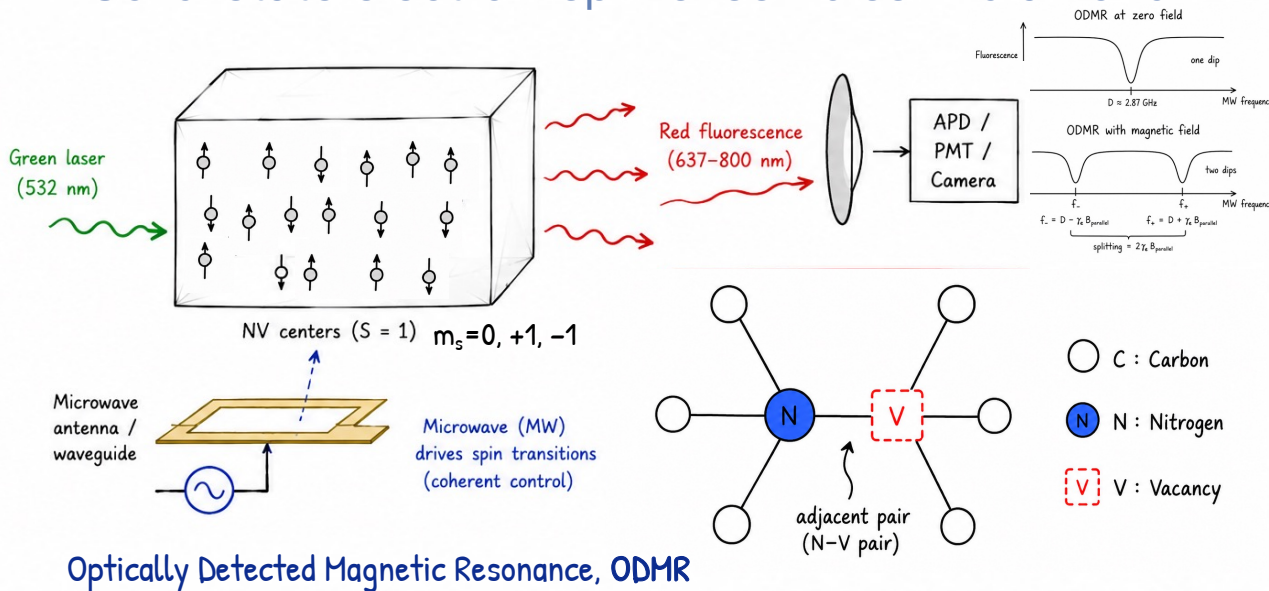
- **Small nuclear magnetic moments**
Intrinsically weaker signals than electron-spin systems
- **Weak thermal polarization**
Often requires strong magnetic fields or hyperpolarization
- **Low-frequency inductive readout limitations**
Small samples are difficult to detect efficiently

Particle physics applications (examples):

- **CASPER axion / CASPER-ZULF DM searches [Prop:18,Exp:19]**
→ resonant pseudo-magnetic spin precession (B_0 scan)
- **Liquid-state nuclear-spin comagnetometer [Exp: 20]**
→ axion-induced anomalous spin coupling
- **Muon $g-2$ magnetic-field metrology [Exp: 21]**
→ precision proton NMR frequency measurement

NV Center Ensembles

Solid-state electron-spin ensembles in diamond



Key characteristics:

- **Optical spin readout**
High-contrast fluorescence enables sensitive detection
- **Room-temperature solid-state operation**
Practical and robust with minimal cryogenic requirements
- **High-density spin ensemble possible**
Many NVs in a small volume → large signal
- **Magnetic imaging with micrometer-scale pixels**
High spatial resolution and wide-field capability

Practical issue:

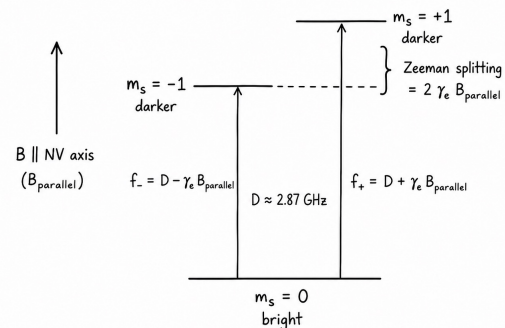
- **Nitrogen-related defects and spin-spin interactions**
Introduce decoherence and background signals
- **Fluorescence collection and contrast are difficult**
Photon shot noise and collection inefficiency limit sensitivity

Particle physics applications (examples):

- **Exotic spin-dependent interactions [Exp: 22]**
→ new physics via spin-coupled backgrounds (single NV)
- **Light dark matter searches with NV centers [Prop: 23]**
→ oscillating pseudo-magnetic or electric fields
- **Axion / dark-photon searches with NV centers [Prop: 24,25]**
→ resonant spin coupling to ultralight fields

Main sensing quantities:

- **Magnetic field B**
→ Zeeman shift of NV electron spin transitions ($\Delta\omega = \gamma_e B$)
- **Electric field E**
→ Stark shift of NV levels ($\Delta\omega = kE$)
- **Temperature T**
→ Zero-field splitting shift ($\Delta D/D$)
- **Strain, Microwave**



DIY Portable NV Center Magnetometer

Pulsed magnetic resonance in diamond with Arduino Uno

A home-made portable device based on Arduino Uno for pulsed magnetic resonance of NV centers in diamond

Cite as: AIP Advances 12, 065321 (2022); doi: 10.1063/5.0089161
Submitted: 6 April 2022 • Accepted: 7 June 2022 •
Published Online: 24 June 2022



C. Mariani,¹⁾ A. Umemoto, and S. Nomura

AFFILIATIONS

Division of Physics, University of Tsukuba, Tennodai 1-1-1, Ibaraki 305-8571, Japan

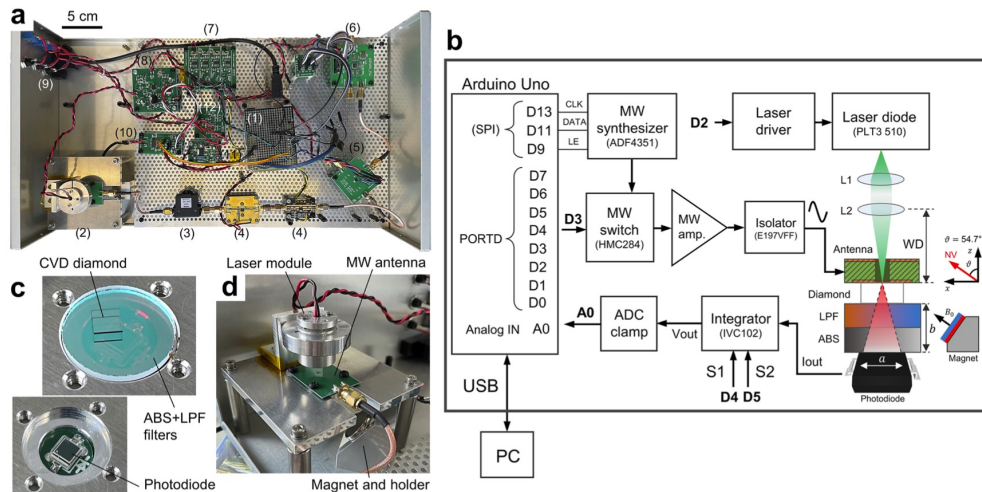


FIG. 1. (a) Interior of the experimental setup: (1) Arduino Uno, (2) sample holder, (3) MW isolator, (4) MW amplifiers, (5) MW switch, (6) MW synthesizer, (7) 5, 3.3 V voltage regulators, (8) laser driver, (9) input of AC/DC converters and USB, (10) switched integrator, (11) ADC clamp, and (12) integrator's ± 12 V regulator. (b) Schematic of the setup. The Arduino board controls the modules by using the digital pins D2–D5, D9, D11, and D13. The laser beam is collimated by a lens (L1) and focused by a lens (L2), with a working distance $WD = 16$ mm from the surface of the diamond. The distance between the diamond and the photodiode (PD) is $b = 2$ mm. The active area of the PD is $a^2 = 2.65 \times 2.65$ mm². (c) Sample holder. The diamond sample with a size of $3 \times 3 \times 0.25$ mm³ is placed on the top of the reflective (LPF) and the absorptive glass (ABS) filters. The PD mounted on a PCB is placed on the back side of the filters and fixed to the aluminum plate with screws. (d) Attachment of the MW antenna and alignment system of the laser diode on the sample holder.

Compact & portable

$20 \times 40 \times 10$ cm³
Weight: ~ 1.8 kg

Low cost

$\sim 98,861$ JPY
(excluding diamond)
 $\sim \$650$ USD

Diamond sample

$\sim 70,000 - 300,000$ JPY ??
(depending on quality)
e.g., CVD type IIa, $3 \times 3 \times 0.25$ mm³

It may be interesting and educational to build a setup like this as a hands-on introduction to NV-center (quantum sensing) experiments.

Summary

Quantum sensors turn weak perturbations into measurable quantum evolution

1. Different implementations use different quantum systems

spins, motional states, Rydberg states, clock transitions, and solid-state defects.

2. The measured quantity is usually a phase, frequency, level shift, or population change

magnetic fields, electric fields, acceleration, rotation, and time/frequency can be sensed.

3. For particle physics, the key is not only sensitivity but also the matching of the signal signature

spin precession → axion / Lorentz tests

frequency shift → ultralight dark matter / varying constants

level shift → fifth forces / isotope-shift anomalies

RF response → dark photon / axion-photon searches

Further Reading

| No. | Type | System | Reference |
|------|------|---------------|---|
| [1] | Exp | Atomic vapor | W. Xiao et al., "Femtotesla Atomic Magnetometer Employing Diffusion Optical Pumping to Search for Exotic Spin-Dependent Interactions," <i>Phys. Rev. Lett.</i> 130 , 143201 (2023). |
| [2] | Exp | Atomic vapor | M. Smiciklas et al., "New Test of Local Lorentz Invariance Using a ^{21}Ne -Rb-K Comagnetometer," <i>Phys. Rev. Lett.</i> 107 , 171604 (2011). |
| [3] | Exp | Atomic vapor | I. M. Bloch et al., "Constraints on axion-like dark matter from a SERF comagnetometer," <i>Nature Communications</i> 14 , 5784 (2023). |
| [4] | Exp | Atomic vapor | C. Abel et al., "Optically pumped Cs magnetometers enabling a high-sensitivity search for the neutron electric dipole moment," <i>Phys. Rev. A</i> 101 , 053419 (2020). |
| [5] | Exp | Cold atoms | P. Asenbaum et al., "Atom-Interferometric Test of the Equivalence Principle," <i>Phys. Rev. Lett.</i> 125 , 191101 (2020). |
| [6] | Exp | Cold atoms | L. Morel et al., "Determination of the fine-structure constant with an accuracy of 81 parts per trillion," <i>Nature</i> 588 , 61–65 (2020). |
| [7] | Prop | Cold atoms | L. Badurina et al., "AION: An Atom Interferometer Observatory and Network," <i>Journal of Cosmology and Astroparticle Physics</i> 2020 (05), 011 (2020). |
| [8] | Prop | Cold atoms | M. Abe et al., "Matter-wave Atomic Gradiometer Interferometric Sensor (MAGIS-100)," <i>Quantum Sci. Technol.</i> 6 , 044003 (2021). |
| [9] | Prop | Trapped ions | A. Ito et al., "Quantum entanglement of ions for light dark matter detection," <i>JHEP</i> 2024 (02), 124 (2024). |
| [10] | Exp | Trapped ions | A. Wilzewski et al., "Nonlinear Calcium King Plot Constrains New Bosons and Nuclear Properties," <i>Phys. Rev. Lett.</i> 134 , 233002 (2025). |
| [11] | Exp | Trapped ions | T. Pruttivarasin et al., "Michelson-Morley analogue for electrons using trapped ions," <i>Nature</i> 517 , 592–595 (2015). |
| [12] | Exp | Trapped ions | L. S. Dreissen et al., "Improved bounds on Lorentz violation from composite pulse Ramsey spectroscopy in a trapped ion," <i>Nature Communications</i> 13 , 7314 (2022). |
| [13] | Prop | Rydberg atoms | E. Graham et al., "Rydberg-atom-based single-photon detection for haloscope axion searches," <i>Phys. Rev. D</i> 109 , 032009 (2024). |
| [14] | Prop | Rydberg atoms | S. Chigusa et al., "Detecting Dark Matter Using Optically Trapped Rydberg Atom Tweezer Arrays," <i>Phys. Rev. Lett.</i> 136 , 151801 (2026). |
| [15] | Exp | Atomic clocks | T. Kobayashi et al., "Search for Ultralight Dark Matter from Long-Term Frequency Comparisons of Optical and Microwave Atomic Clocks," <i>Phys. Rev. Lett.</i> 129 , 241301 (2022). |
| [16] | Exp | Atomic clocks | C. J. Kennedy et al., "Precision Metrology Meets Cosmology: Improved Constraints on Ultralight Dark Matter from Atom-Cavity Frequency Comparisons," <i>Phys. Rev. Lett.</i> 125 , 201302 (2020). |
| [17] | Prop | Atomic clocks | A. Derevianko and M. Pospelov, "Hunting for topological dark matter with atomic clocks," <i>Nature Physics</i> 10 , 933–936 (2014). |
| [18] | Prop | NMR | D. Budker et al., "Proposal for a Cosmic Axion Spin Precession Experiment," <i>Phys. Rev. X</i> 4 , 021030 (2014). |
| [19] | Exp | NMR | A. Garcon et al., "Constraints on bosonic dark matter from ultralow-field nuclear magnetic resonance," <i>Science Advances</i> 5 , eaax4539 (2019). |
| [20] | Exp | NMR | T. Wu et al., "Search for Axionlike Dark Matter with a Liquid-State Nuclear Spin Comagnetometer," <i>Phys. Rev. Lett.</i> 122 , 191302 (2019). |
| [21] | Exp | NMR | T. Albahri et al. (Muon g-2 Collaboration), "Magnetic-field measurement and analysis for the Muon g-2 Experiment at Fermilab," <i>Phys. Rev. A</i> 103 , 042208 (2021). |
| [22] | Exp | NV centers | X. Rong et al., "Searching for an exotic spin-dependent interaction with a single electron-spin quantum sensor," <i>Nature Communications</i> 9 , 739 (2018). |
| [23] | Prop | NV centers | S. Chigusa et al., "Light dark matter search with nitrogen-vacancy centers in diamond," <i>JHEP</i> 03 , 083 (2025). |
| [24] | Prop | NV centers | S. Chigusa et al., "Nuclear spin metrology with nitrogen vacancy center in diamond," <i>Phys. Rev. D</i> 111 , 075028 (2025). |
| [25] | Prop | NV centers | A. Guo et al., "Searching for exotic spin-dependent interactions with diamond-based vector magnetometer," <i>Phys. Rev. D</i> 109 , 055034 (2024). |